

Research Report

Symmetric and Profound Monoaminergic Degeneration in Parkinson's Disease with Premotor REM Sleep Behavior Disorder

Kyung Ah Woo^a, Han-Joon Kim^{a,*}, Jung Hwan Shin^a, Kangyoung Cho^b, Hongyoon Choi^b
and Beomseok Jeon^a

^aDepartment of Neurology, Seoul National University Hospital, Seoul National University College of Medicine, Seoul, Korea

^bDepartment of Nuclear Medicine, Seoul National University Hospital, Seoul National University College of Medicine, Seoul, Korea

Accepted 18 March 2024

Pre-press 12 April 2024

Published 4 June 2024

Abstract.

Background: Rapid eye movement sleep behavior disorder (RBD) may precede or follow motor symptoms in Parkinson's disease (PD). While over 70% of idiopathic RBD cases phenoconvert within a decade, a small subset develops PD after a more extended period or remains nonconverted. These heterogeneous manifestations of RBD in PD prompt subtype investigations. Premotor RBD may signify “body-first” PD with bottom-up, symmetric synucleinopathy propagation.

Objective: Explore brainstem and nigrostriatal monoaminergic degeneration pattern differences based on premotor RBD presence and duration in *de novo* PD patients.

Methods: In a cross-sectional analysis of *de novo* PD patients ($n = 150$) undergoing FP-CIT PET and RBD Single-Question Screen, the cohort was categorized into groups with and without premotor RBD ($PD^{RBD+/-}$), with further classification of PD^{RBD+} based on a 10-year duration of premotor RBD. Analysis of FP-CIT binding in the striatum and pons, striatal asymmetry, and striatum-to-pons ratios compared patterns of nigrostriatal and brainstem monoaminergic degeneration.

Results: PD^{RBD+} exhibited more severe and symmetrical striatal dopaminergic denervation compared to PD^{RBD-} , with the difference in severity accentuated in the least-affected hemisphere. The $PD^{RBD+ < 10Y}$ subgroup displayed the most prominent striatal symmetry, supporting a more homogeneous “body-first” subtype. Pontine uptakes remained lower in PD^{RBD+} even after adjusting for striatal uptake, suggesting early degeneration of pontine monoaminergic nuclei.

Conclusions: Premotor RBD in PD is associated with severe, symmetrical nigrostriatal and brainstem monoaminergic degeneration, especially in cases with PD onset within 10 years of RBD. This supports the concept of a “widespread, bottom-up” pathophysiological mechanism associated with premotor RBD in PD.

Keywords: Parkinson's disease, REM sleep behavior disorder, Lewy body disease, positron emission tomography

INTRODUCTION

Idiopathic rapid eye movement (REM) sleep behavior disorder (iRBD), characterized by dream enactment behavior and loss of REM sleep atonia, serves as a robust prodromal indicator for Parkinson's

*Correspondence to: Han-Joon Kim, MD, PhD, Department of Neurology, Seoul National University College of Medicine, 101 Daehak-ro, Jongno-gu, Seoul 03080, South Korea. Tel.: +82 2 2072 2278; Fax: +82 2 3672 7553; E-mail: movement@snu.ac.kr.

disease (PD), with approximately 70% developing synucleinopathy within 10 years [1–3]. However, from the PD standpoint, premotor RBD is only observed in a subset of newly diagnosed patients, with an estimated prevalence ranging from 25% to 40%, and many PD patients experience RBD after the onset of motor symptoms [4–7].

The heterogeneous manifestation of RBD in PD has prompted efforts to subtype the disease based on its presence. In PD, the co-presence of RBD is associated with a ‘diffuse and/or malignant’ subtype of disease, along with a higher risk of dementia, psychiatric comorbidity, and autonomic dysfunction [8–12]. The recent α -Synuclein Origin and Connectome (SOC) Model of PD suggests that premotor RBD signifies a “body-first” PD subtype characterized by a bottom-up spread of peripheral synucleinopathy through the brainstem [13]. This subtype is expected to exhibit a more symmetrical nigrostriatal degeneration pattern compared to the “brain-first” subtype, where pathology likely begins at a unilateral site inside the brain.

Meanwhile, a small yet distinct subgroup of longstanding iRBD patients, either undergoing phenocconversion after more than 10 years or remaining nonconverted for an extended period, is consistently observed across multiple prospective studies [14, 15]. However, considering the anatomical proximity of RBD’s key brainstem neuronal network to nigral dopaminergic neurons [16], the remarkably prolonged lag period between RBD and motor parkinsonism raises questions about whether an alternative neurodegenerative pathomechanism should be contemplated [17] rather than the straightforward progression of premotor RBD into “body-first” PD, at least in some instances among these long-lagged PD cases.

Given these considerations, in a cohort of newly diagnosed PD patients undergoing FP-CIT positron emission tomography (PET), we aimed to analyze potential differences in brain monoaminergic denervation patterns based on the presence and temporal profile of premotor RBD. Specifically, we hypothesized that, in the premotor RBD group, the proposed pathomechanism of “body-first” PD would lead to (i) more symmetrical nigrostriatal dopaminergic denervation and (ii) more profound pontine monoaminergic degeneration, both in terms of absolute values and relative ratios to nigrostriatal denervation, as the pathological propagation is suggested to be ‘bottom-up’ [13]. Furthermore, we hypothesized that the symmetric nigrostriatal and

severe pontine denervation patterns expected for “body-first” PD would be more pronounced in the subgroup with a temporal gap of less than 10 years between the onset of RBD symptoms and motor parkinsonism compared to the group with an extensive lag period.

MATERIALS AND METHODS

Study participants

The medical records of consecutive patients diagnosed with *de novo* PD at the Movement Disorders Clinic of Seoul National University Hospital between 2013 and 2022 were retrospectively reviewed. The inclusion criteria comprised patients who met the clinical criteria for probable or established PD and had undergone ^{18}F -FP-CIT PET scan at diagnosis [18]. The diagnosis was established by a movement disorders specialist (HJ Kim). To retrospectively ensure the reliability of the PD diagnosis, only patients with at least 3 years of disease duration at the time of chart review were included. Additionally, in order to reflect the neurodegenerative pattern at disease onset and to minimize the variability of disease duration and age among groups, only patients who had undergone PET scan within 2 years of onset and were aged 60 to 80 years at scan were included.

The study protocol was approved by the Institutional Review Board (IRB) of the Seoul National University Hospital (No. 2201-085-1290). Informed consent was waived by the IRB due to the retrospective nature of the study.

Clinical information and assessment for probable premotor RBD

Demographic information on sex, age at PD onset, and age at PET scan was collected for all participants. At the time of diagnosis, clinical interview was conducted to screen for a history of RBD. Specifically, participants and their bed-sharing caregivers were asked—both of them had to be able to provide an answer—if they had ever been told that (or ever appeared to) “act out his/her dreams while sleeping, i.e., punched or flailed arms in the air, shouted or screamed [19].” Those who answered “yes” for the participant were deemed to have probable RBD and were further questioned about the onset of such dream enactment behaviors. Participants were grouped based on the presence or absence of probable RBD at the time of PD onset based on clinical

history. The duration of probable RBD preceding PD, i.e., the interval between the onsets of probable RBD and PD, was calculated in years.

PET acquisition and processing

The participants underwent ^{18}F -FP-CIT PET scans at drug-naïve status. For ^{18}F -FP-CIT PET study, CT scans were conducted for attenuation correction, and subsequent PET emission scans were carried out 120 min after injecting ^{18}F -FP-CIT (185 MBq) using dedicated PET/CT scanners from Siemens Healthineers (Biograph true point with true V or Biograph mCT 40 or Biograph mCT 64; Erlangen, Germany). The PET images were reconstructed using the ordered-subset expectation maximization algorithm with 21 subsets and 6 iterations. The finally reconstructed image matrix size was 400×400 .

These PET images were spatially registered to a previously developed in-house MNI FP-CIT PET template with a voxel size of $2 \times 2 \times 2$ mm [20, 21]. The nonlinear spatial registration was performed using rigid and affine transformation followed by Symmetric Diffeomorphic Registration (SyN) as a nonlinear registration implemented in Dipy package (version 1.1.1, <https://dipy.org/>) [22]. The registered images were smoothed by an additional Gaussian filter with full-width at half maximum of 10 mm.

For quantification of FP-CIT standardized uptake ratio (SUR) in each volume of interest (VOI), the standardized uptake value of the specific VOI was divided by the value of the occipital cortex as the reference region. The VOIs of occipital cortex as well as putamen and caudate nucleus were delineated by predefined anatomic atlas (AAL, Automated Anatomical Labeling) [23]. The brainstem VOIs for the rostral pons, hereafter pons, was drawn manually on the FP-CIT PET template overlaid with the template MRI according to the previous literature [24, 25], using MRICron (<https://www.nitrc.org/projects/mricron>). In addition, to define ventral striatum, additional striatal predefined VOIs were used [26]. Pons and whole striatum were extracted as a single region of the entire corresponding area without distinguishing between the bilateral hemispheres, respectively. The SUR of the least-affected hemisphere (LAH) or the most-affected hemisphere (MAH) was also computed for each striatal VOI [27]. This involved selecting the higher value between the bilateral hemisphere values for LAH and the lower value for MAH in each striatal VOI.

The asymmetry index and the striatum-to-pons ratios

The asymmetry index (AI) between the ^{18}F -FP-CIT PET SURs of bilateral striatum in each VOI was calculated as in previous studies [28, 29]: $[(a-b)/(a+b)] \times 2 \times 100$, with a and b representing the two different sides' SURs of each VOI. The striatum-to-pons ratios were calculated as (mean SUR value of each striatal VOI or the whole striatal SUR)/(pontine SUR).

Statistical analysis

Comparison of mean between two groups was performed using the two-sample t test and Pearson chi-squared test as appropriate. One-way analysis of variance (ANOVA) was used to compare the mean levels in three or more groups. For the correlational analysis between putaminal SUR and AI, we used Pearson's correlation analysis. Statistical threshold was set at $p < 0.05$ using the false discovery rate (FDR) correction for multiple comparisons across VOIs. Statistical analysis was performed using IBM SPSS version 24 (Armonk, NY; IBM Corp) and Graphpad Prism 10.0.

RESULTS

A total of 150 subjects with *de novo* PD were included in this study. The demographics and clinical characteristics are presented in Table 1. The mean age at PD onset was 66.88 ± 5.667 years, and at PET scan 67.98 ± 5.536 years. Ninety-eight subjects had probable RBD at the time of PD onset ($\text{PD}^{\text{RBD}+}$), 43 of whom reported that the onset of RBD preceded that of PD by 10 years or more ($\text{PD}^{\text{RBD}+\geq 10\text{Y}}$).

Striatal dopaminergic asymmetry and striatum-to-pons ratios of monoaminergic denervation by probable premotor RBD in PD

Although no statistically significant differences were observed between the $\text{PD}^{\text{RBD}+}$ and $\text{PD}^{\text{RBD}-}$ groups concerning sex, age at PD onset, and age at PET imaging, distinctions emerged in striatal and pontine FP-CIT uptakes, demonstrating significantly lower values in both the striatum VOIs and the pons in the $\text{PD}^{\text{RBD}+}$ group ($p_{\text{FDR}} < 0.05$). Analyzing striatal asymmetry between groups revealed a more symmetric pattern of FP-CIT binding in the putamen ($p_{\text{FDR}} < 0.001$) and the caudate nucleus

Table 1
Demographics and ^{18}F -FP-CIT PET findings in patients with *de novo* PD, with or without preceding history of probable RBD

	PD ^{RBD-}	PD ^{RBD+}	<i>p</i>
Sex	24/28	56/42	0.201
Age at PD onset, y	66.50 (5.338)	67.05 (5.702)	0.544
Age at PET imaging, y	67.67 (5.272)	68.14 (5.691)	0.623
Disease duration, y	1.173 (0.648)	1.061 (0.715)	0.348
^{18}F-FP-CIT SUR			
Pons	2.165 (0.470)	1.841 (0.570)	<0.001
Caudate, mean	3.537 (0.662)	3.313 (0.536)	0.026
Putamen, mean	3.539 (0.567)	3.275 (0.517)	0.005
Ventral striatum, mean	1.699 (0.303)	1.587 (0.266)	0.021
Whole Striatum	3.536 (0.599)	3.292 (0.510)	0.010
^{18}F-FP-CIT SUR AI's			
AI, caudate	7.221 (4.788)	5.296 (4.696)	0.019
AI, putamen	16.042 (8.523)	10.323 (9.242)	<0.001
AI, ventral striatum	26.196 (9.591)	24.910 (8.296)	0.394
^{18}F-FP-CIT SUR striatum-to-pons ratios			
Caudate/Pons	1.723 (0.560)	1.999 (0.761)	0.013
Putamen/Pons	1.730 (0.563)	1.966 (0.703)	0.027
Ventral striatum/Pons	0.832 (0.286)	0.958 (0.370)	0.022
Whole Striatum/Pons	1.726 (0.556)	1.981 (0.726)	0.018
^{18}F-FP-CIT SUR in the most- and least-affected-hemispheres			
Putamen			
MAH	3.252 (0.532)	3.101 (0.484)	0.083
LAH	3.825 (0.643)	3.448 (0.597)	<0.001
Caudate			
MAH	3.412 (0.659)	3.226 (0.530)	0.063
LAH	3.663 (0.675)	3.400 (0.554)	0.011
Ventral Striatum			
MAH	1.476 (0.279)	1.389 (0.244)	0.053
LAH	1.922 (0.348)	1.785 (0.304)	0.013

SUR, standardized uptake ratio; AI, asymmetry index *p*-values that remained <0.05 after correction for multiple comparisons are highlighted in bold.

($p_{\text{FDR}} < 0.05$) in the PD^{RBD+} group compared to the PD^{RBD-} group, while ventral striatal AIs did not exhibit significant differences (Fig. 1a). Furthermore, the PD^{RBD+} group exhibited a higher striatum-to-pons ratio of FP-CIT binding in all striatal VOIs, i.e., putamen/pons, compared to the PD^{RBD-} group ($p_{\text{FDR}} < 0.05$; Fig. 1b), indicating a relatively pronounced decrease in pontine SURs over the striatum in the PD^{RBD+} group.

Comparison of striatal dopaminergic denervation in the MAH and LAH by premotor RBD

Analysis of the MAH and LAH striatal SURs of the subjects revealed further distinctions between the PD^{RBD+} and PD^{RBD-} groups (Table 1). The PD^{RBD+} group exhibited significantly lower SURs in the LAH putamen, caudate, and ventral striatum compared to the PD^{RBD-} group, while SURs in the

MAHs within each striatal VOI did not differ significantly between the two groups. Further comparisons, controlling for individual MAH SURs in each VOI, continued to demonstrate lower LAH uptakes in the putamen ($p = 0.0002$) and caudate ($p = 0.005$) in the PD^{RBD+} group. A significant positive correlation was identified between the putaminal AI and the putaminal FP-CIT SUR in the LAH (Pearson's $r = 0.451$, $p < 0.001$; Fig. 1c), but not with the MAH.

Comparison of striatal degeneration and asymmetry based on the duration of premotor RBD

The PD^{RBD+} group was further categorized based on the duration of premotor RBD, including the PD^{RBD+ < 10Y} group with less than 10 years of premotor RBD duration and the PD^{RBD+ ≥ 10Y} group with longstanding premotor RBD of 10 years or more (Supplementary Table 1). Both groups exhib-

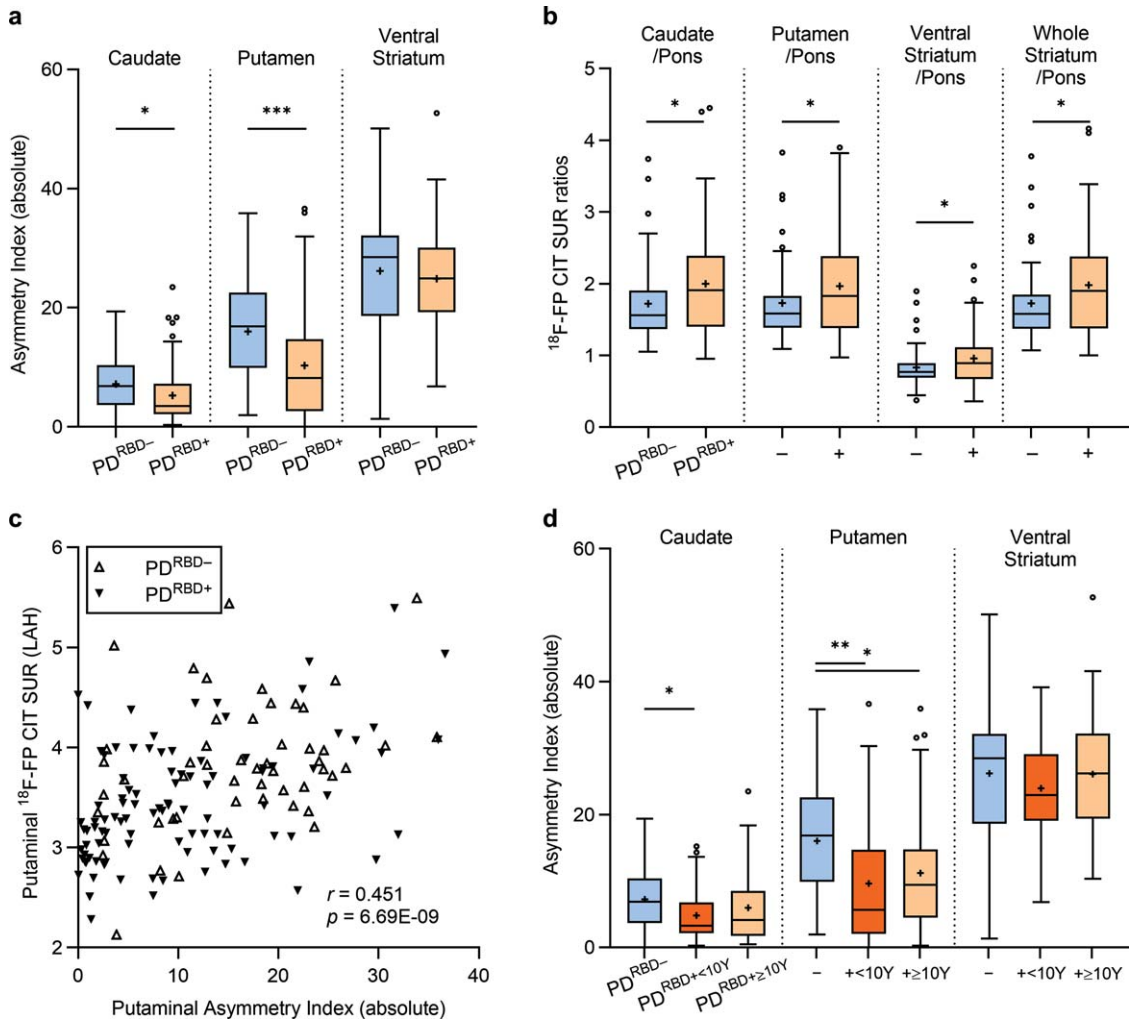


Fig. 1. Striatal asymmetry and striatum-to-pons ratios of monoaminergic degeneration in drug-naïve Parkinson's disease stratified by premotor RBD. The PD^{RBD+} group displays (a) a more symmetric nigrostriatal degeneration and (b) higher striatum-to-pons ratios of FP-CIT binding, indicating a marked pontine monoaminergic degeneration compared to the PD^{RBD-} group. (c) Putamenal asymmetry is primarily driven by the severity of least-affected hemisphere (LAH) degeneration. (d) The symmetric degeneration pattern of the striatum is more pronounced in the subgroup of PD^{RBD+} with less than 10 years of premotor RBD history.

ited lower pontine FP-CIT uptakes compared to the PD^{RBD-} group (*post hoc* $p_{FDR} = 0.022$ for both). However, putamenal FP-CIT binding was reduced only in the PD^{RBD+<10Y} group compared to the PD^{RBD-} group (*post hoc* $p_{FDR} = 0.048$). No significant differences were found in caudate uptake among the three groups.

The PD^{RBD+<10Y} group also displayed a prominently symmetric denervation pattern in the putamen and the caudate nucleus compared to the PD^{RBD-} group (*post hoc* $p_{FDR} = 0.003$ and 0.021 , respectively; Fig. 1d). In contrast, the PD^{RBD+≥10Y} group dis-

played relative symmetry only in the putamen than the PD^{RBD-} group (*post hoc* $p_{FDR} = 0.028$), without a significant symmetry difference in the caudate nucleus. No additional differences in the striatum-to-pons ratios were found among the PD^{RBD-}, the PD^{RBD+≥10Y}, and the PD^{RBD+<10Y} groups.

When comparing asymmetry between the two groups, arithmetically higher asymmetries were noted in the PD^{RBD+≥10Y} than the PD^{RBD+<10Y} group in all striatal VOIs, but these differences did not reach statistical significance (Supplementary Table 1).

DISCUSSION

In this cohort of *de novo* PD patients, our investigation reveals that individuals with probable premotor RBD (PD^{RBD+}) exhibit significantly more symmetrical striatal dopaminergic denervation than those without premotor RBD (PD^{RBD-}). The relatively higher severity of LAH denervation in PD^{RBD+}, compared to PD^{RBD-}, contributes to the symmetry, while MAH severity is comparable between the two groups. Within the PD^{RBD+} subgroups, individuals with a premotor RBD duration of less than 10 years exhibit a particularly more symmetrical pattern than the PD^{RBD-} group. Additionally, the PD^{RBD+} group shows lower pontine FP-CIT uptake than the PD^{RBD-} group, even after adjusting for striatal uptake (i.e., a higher striatum/pons ratio), suggesting a link between premotor RBD and early degeneration of the pontine monoaminergic nuclei.

We observe profound degeneration of the striatal LAH in the *de novo* PD^{RBD+} group, despite comparable severity in the MAHs when compared to the PD^{RBD-} group. This aligns with the expectations for “body-first” PD: a symmetric and higher overall burden of nigrostriatal degeneration at the time of diagnosis [13, 30]. The SOC model postulates that the initial gastrointestinal pathology in the “body-first” subtype ascends via bilateral dorsal motor nuclei of the vagus, resulting in an extended prodromal phase and a more extensive accumulation of bilateral pathology until motor onset [13]. Given the relatively stereotypical trajectory of dopamine degeneration once initiated [31–34], the comparable severity in the MAHs indicates that the initial dopamine degeneration likely started at similar time-points in the past across the PD^{RBD+} and PD^{RBD-} groups. However, in the PD^{RBD+} group, it may have progressed more symmetrically, leading to a greater involvement of the LAH at the diagnostic stage. Previous research reported symmetric degeneration in the PD^{RBD+} group compared to the PD^{RBD-} group, but as the groups significantly differed in ages [35], the ability to compare the absolute severity of neurodegeneration in the LAH or the MAH was constrained. Our cohort, comprising age- and disease-duration-matched groups, each with over 40 subjects, enabled a quantitative comparison of dopaminergic neurodegeneration and symmetry in the postulated “body-first” and “brain-first” groups of *de novo* patients. Our findings also align with the pathological observation that the extent and density

of synuclein pathology are higher in PD patients with probable RBD [36].

The extrastriatal investigation of FP-CIT binding reveals reduced pontine SURs in the PD^{RBD+} group, further supporting the assumptions in the SOC model that “body-first” PD has more damage in the pontine modulatory neurotransmitter systems, such as the raphe nucleus (RN) or the locus coeruleus (LC), in the early stages [13]. FP-CIT has affinity for serotonin (SERT) and noradrenaline transporters (NAT) in addition to dopamine transporters (DAT) [37]. Therefore, its binding at the pons level, where DATs are scarce, mainly reflects the somatodendritic availability of SERTs in the RN or the NATs in the LC, while at the striatal level, it reflects the predominant DATs at the nigral nerve terminals [37–39]. The higher striatum-to-pons ratio of SURs in the PD^{RBD+} group further supports the notion that degeneration of pontine monoaminergic nuclei is more severe, even after adjusting for the degree of nigrostriatal dopaminergic degeneration. Apart from the SOC model, this aligns with classical evidence that brainstem serotonergic and noradrenergic alterations contribute to RBD pathogenesis, along with cholinergic systems [16].

Our results illustrate that the striatal DAT symmetry of PD^{RBD+} is particularly pronounced in the PD^{RBD+<10Y} subgroup. Large-scale multicenter studies on iRBD report overall phenoconversion rates of 70–75% after 10–12 years [1, 3], indicating that at least 10% may remain nonconverted after a decade. We specifically focused on this minority of RBD patients with a prolonged lag period between the RBD and motor parkinsonism [17]. We hypothesized that this group may comprise a mix of patients, including 1) those with a markedly gradual progression of prodromal body-first parkinsonian pathology, and 2) those with non-progressive RBD and an independent development of brain-first PD. The results, indicating the most prominent “body-first-like” striatal symmetry trend in the PD^{RBD+<10Y} group, may support this hypothesis. Our findings suggest a possibility that a subset of these patients may experience a predominant “brain-first” pathomechanism independently occurring from RBD, because otherwise the PD^{RBD+≥10Y} group should show reduced putaminal FP-CIT binding and symmetry as in the PD^{RBD+<10Y} group. As part of ongoing efforts to subtype PD based on premotor RBD, considering the duration of preceding RBD may prove beneficial in identifying patient subgroups at a higher risk of faster progression and/or dementia.

Some limitations of our study should be addressed. Firstly, the absence of video polysomnography (PSG) confirmation of RBD poses a limitation. The RBD Single-Question Screen, the RBD1Q, is a versatile tool to screen for RBD in the clinics and poses an estimated specificity of 87% and sensitivity of 94% for PSG-confirmed RBD [19]. Still, the proportion of RBD-positive cases at diagnosis in our study was relatively higher than previously reported figures [4]. This could have been influenced by the questionnaire-based nature of the data and our requirement for both the patient and the bed partner to be present to answer the questionnaire. In other words, the inclusion of false-positive cases with secondary RBD and exclusion of cases without a bed partner, with or without RBD, might have impacted the rate in either way. We speculate that future investigations in a PSG-confirmed cohort may settle these limitations, providing valuable insights and validating our findings. Additionally, the inclusion criteria for PD duration and age at scan, implemented to control group differences, might have unintentionally affected the positivity rate. Second, the accuracy of the reported time of RBD onset may have been affected by recall bias. However, it is essential to note that 1) bed partners confirmed the onset of RBD in all cases, enhancing the reliability of reported onset times, and 2) the majority of cases (87.3%) specifying an RBD–PD interval of less than 10 years clarified that it fell within the 1–5-year range. This suggests a lower likelihood of confusion between durations less than 10 years and more than 10 years by patients and their bed partners. Thirdly, the absence of quantitative evaluation data for motor and nonmotor symptoms at the time of PET scan hinders the exploration of clinical correlations. Lastly, as the VOIs were delineated on the PET images using the template, and individual MRIs were not available, unrecognized atrophy could have influenced the FP-CIT SURS, particularly in the brainstem. A structural evaluation combined with PET analysis in the future is warranted.

In conclusion, our study highlights the association between premotor RBD and pronounced, symmetric degeneration of nigrostriatal dopaminergic nerve terminals in *de novo* PD, particularly evident in individuals developing PD within 10 years of RBD onset. Furthermore, premotor RBD is correlated with significant degeneration of the pontine monoaminergic nuclei. These findings indicate that premotor RBD in PD is linked to a subtype of the disease characterized by a more profound neurodegeneration, potentially

suggesting a “widespread, bottom-up” pathophysiological mechanism.

ACKNOWLEDGMENTS

The authors have no acknowledgments to report.

FUNDING

This study was supported by grant No. 0420230280 from the SNUH Research Fund and the National Research Foundation of Korea (NRF) grant funded by the Korea government (MSIT) (No. 2022R1A2C2091254).

CONFLICT OF INTEREST

The authors have no conflict of interest to report.

DATA AVAILABILITY

The data supporting the findings of this study are available on request from the corresponding author.

SUPPLEMENTARY MATERIAL

The supplementary material is available in the electronic version of this article: <https://dx.doi.org/10.3233/JPD-230459>.

REFERENCES

- [1] Zhang H, Iranzo A, Hogl B, Arnulf I, Ferini-Strambi L, Manni R, Miyamoto T, Oertel WH, Dauvilliers Y, Ju YE, Puligheddu M, Sonka K, Pelletier A, Montplaisir JY, Stefani A, Ibrahim A, Frauscher B, Leu-Semenescu S, Zucconi M, Terzaghi M, Miyamoto M, Janzen A, Figorilli M, Fantini ML, Postuma RB (2022) Risk factors for phenoconversion in rapid eye movement sleep behavior disorder. *Ann Neurol* **91**, 404-416.
- [2] Berg D, Postuma RB, Adler CH, Bloem BR, Chan P, Dubois B, Gasser T, Goetz CG, Halliday G, Joseph L, Lang AE, Liepelt-Scarfone I, Litvan I, Marek K, Obeso J, Oertel W, Olanow CW, Poewe W, Stern M, Deuschl G (2015) MDS research criteria for prodromal Parkinson's disease. *Mov Disord* **30**, 1600-1611.
- [3] Postuma RB, Iranzo A, Hu M, Hogl B, Boeve BF, Manni R, Oertel WH, Arnulf I, Ferini-Strambi L, Puligheddu M, Antelmi E, Cochen De Cock V, Arnaldi D, Mollenhauer B, Videnovic A, Sonka K, Jung KY, Kunz D, Dauvilliers Y, Provini F, Lewis SJ, Buskova J, Pavlova M, Heidebreder A, Montplaisir JY, Santamaria J, Barber TR, Stefani A, St Louis EK, Terzaghi M, Janzen A, Leu-Semenescu S, Plazzi G, Nobili F, Sixel-Doering F, Dusek P, Bes F, Cortelli P, Ehgoetz Martens K, Gagnon JF, Gaig C, Zucconi M, Trenkwalder C, Gan-Or Z, Lo C, Rolinski M, Mahlknecht

- P, Holzknrecht E, Boeve AR, Teigen LN, Toscano G, Mayer G, Morbelli S, Dawson B, Pelletier A (2019) Risk and predictors of dementia and parkinsonism in idiopathic REM sleep behaviour disorder: A multicentre study. *Brain* **142**, 744-759.
- [4] Sixel-Doring F, Trautmann E, Mollenhauer B, Trenkwalder C (2014) Rapid eye movement sleep behavioral events: A new marker for neurodegeneration in early Parkinson disease? *Sleep* **37**, 431-438.
- [5] Zimansky L, Muntean ML, Leha A, Mollenhauer B, Trenkwalder C, Sixel-Doring F (2021) Incidence and progression of rapid eye movement behavior disorder in early Parkinson's disease. *Mov Disord Clin Pract* **8**, 534-540.
- [6] Sixel-Doring F, Muntean ML, Peterson D, Leha A, Lang E, Mollenhauer B, Trenkwalder C (2023) The increasing prevalence of REM sleep behavior disorder with Parkinson's disease progression: A polysomnography-supported study. *Mov Disord Clin Pract* **10**, 1769-1776.
- [7] Alariste-Booth V, Rodriguez-Violante M, Camacho-Ordóñez A, Cervantes-Arriaga A (2015) Prevalence and correlates of sleep disorders in Parkinson's disease: A polysomnographic study. *Arq Neuropsiquiatr* **73**, 241-245.
- [8] Postuma RB, Gagnon JF, Vendette M, Montplaisir JY (2009) Markers of neurodegeneration in idiopathic rapid eye movement sleep behaviour disorder and Parkinson's disease. *Brain* **132**, 3298-3307.
- [9] Postuma RB, Montplaisir J, Lanfranchi P, Blais H, Rompre S, Colombo R, Gagnon JF (2011) Cardiac autonomic denervation in Parkinson's disease is linked to REM sleep behavior disorder. *Mov Disord* **26**, 1529-1533.
- [10] Sixel-Doring F, Trautmann E, Mollenhauer B, Trenkwalder C (2011) Associated factors for REM sleep behavior disorder in Parkinson disease. *Neurology* **77**, 1048-1054.
- [11] Postuma RB, Bertrand JA, Montplaisir J, Desjardins C, Vendette M, Rios Romenets S, Panisset M, Gagnon JF (2012) Rapid eye movement sleep behavior disorder and risk of dementia in Parkinson's disease: A prospective study. *Mov Disord* **27**, 720-726.
- [12] Shin C, Kim SI, Park SH, Shin JH, Lee CY, Yang HK, Lee HJ, Kong SH, Suh YS, Kim HJ, Jeon B (2022) Sensitivity of detecting alpha-synuclein accumulation in the gastrointestinal tract and tissue volume examined. *J Mov Disord* **15**, 264-268.
- [13] Borghammer P (2021) The alpha-Synuclein Origin and Connectome Model (SOC Model) of Parkinson's disease: Explaining motor asymmetry, non-motor phenotypes, and cognitive decline. *J Parkinsons Dis* **11**, 455-474.
- [14] Iranzo A, Stefani A, Serradell M, Marti MJ, Lomena F, Mhlknecht P, Stockner H, Gaig C, Fernandez-Arcos A, Poewe W, Tolosa E, Hogl B, Santamaria J, SINBAR (Sleep Innsbruck Barcelona) group (2017) Characterization of patients with longstanding idiopathic REM sleep behavior disorder. *Neurology* **89**, 242-248.
- [15] Yao C, Fereshtehnejad SM, Dawson BK, Pelletier A, Gan-Or Z, Gagnon JF, Montplaisir JY, Postuma RB (2018) Longstanding disease-free survival in idiopathic REM sleep behavior disorder: Is neurodegeneration inevitable? *Parkinsonism Relat Disord* **54**, 99-102.
- [16] Boeve BF, Silber MH, Saper CB, Ferman TJ, Dickson DW, Parisi JE, Benarroch EE, Ahlskog JE, Smith GE, Caselli RC, Tippman-Peikert M, Olson EJ, Lin SC, Young T, Wszolek Z, Schenck CH, Mahowald MW, Castillo PR, Del Tredici K, Braak H (2007) Pathophysiology of REM sleep behaviour disorder and relevance to neurodegenerative disease. *Brain* **130**, 2770-2788.
- [17] Bohnen NI, Postuma RB (2020) Body-first versus brain-first biological subtyping of Parkinson's disease. *Brain* **143**, 2871-2873.
- [18] Postuma RB, Berg D, Stern M, Poewe W, Olanow CW, Oertel W, Obeso J, Marek K, Litvan I, Lang AE, Halliday G, Goetz CG, Gasser T, Dubois B, Chan P, Bloem BR, Adler CH, Deuschl G (2015) MDS clinical diagnostic criteria for Parkinson's disease. *Mov Disord* **30**, 1591-1601.
- [19] Postuma RB, Arnulf I, Hogl B, Iranzo A, Miyamoto T, Dauvilliers Y, Oertel W, Ju YE, Puligheddu M, Jennum P, Pelletier A, Wolfson C, Leu-Semenescu S, Frauscher B, Miyamoto M, Cohen De Cock V, Unger MM, Stiasny-Kolster K, Fantini ML, Montplaisir JY (2012) A single-question screen for rapid eye movement sleep behavior disorder: A multicenter validation study. *Mov Disord* **27**, 913-916.
- [20] Kim YI, Im HJ, Paeng JC, Lee JS, Eo JS, Kim DH, Kim EE, Kang KW, Chung JK, Lee DS (2012) Validation of simple quantification methods for (18)F-FP-CIT PET using automatic delineation of volumes of interest based on statistical probabilistic anatomical mapping and isocontour margin setting. *Nucl Med Mol Imaging* **46**, 254-260.
- [21] Choi H, Cheon GJ, Kim HJ, Choi SH, Lee JS, Kim YI, Kang KW, Chung JK, Kim EE, Lee DS (2014) Segmentation-based MR attenuation correction including bones also affects quantitation in brain studies: An initial result of 18F-FP-CIT PET/MR for patients with parkinsonism. *J Nucl Med* **55**, 1617-1622.
- [22] Avants BB, Epstein CL, Grossman M, Gee JC (2008) Symmetric diffeomorphic image registration with cross-correlation: Evaluating automated labeling of elderly and neurodegenerative brain. *Med Image Anal* **12**, 26-41.
- [23] Tzourio-Mazoyer N, Landeau B, Papathanassiou D, Crivello F, Etard O, Delcroix N, Mazoyer N, Joliot M (2002) Automated anatomical labeling of activations in SPM using a macroscopic anatomical parcellation of the MNI MRI single-subject brain. *Neuroimage* **15**, 273-289.
- [24] Nam SB, Kim K, Kim BS, Im HJ, Lee SH, Kim SJ, Kim IJ, Pak K (2018) The effect of obesity on the availabilities of dopamine and serotonin transporters. *Sci Rep* **8**, 4924.
- [25] Jhoo JH, Yoon IY, Kim YK, Chung S, Kim JM, Lee SB, Kim TH, Moon SH, Kim SE, Kim KW (2010) Availability of brain serotonin transporters in patients with restless legs syndrome. *Neurology* **74**, 513-518.
- [26] Parkes L, Fulcher BD, Yucel M, Fornito A (2017) Transcriptional signatures of connectomic subregions of the human striatum. *Genes Brain Behav* **16**, 647-663.
- [27] Arnaldi D, Chincarin A, Hu MT, Sonka K, Boeve B, Miyamoto T, Puligheddu M, De Cock VC, Terzaghi M, Plazzi G, Tachibana N, Morbelli S, Rolinski M, Dusek P, Lowe V, Miyamoto M, Figorilli M, Verbizier D, Bossert I, Antelmi E, Meli R, Barber TR, Trnka J, Miyagawa T, Serra A, Pizzi F, Bauckneht M, Bradley KM, Zogala D, McGowan DR, Jordan L, Manni R, Nobili F (2021) Dopaminergic imaging and clinical predictors for phenocopy of REM sleep behaviour disorder. *Brain* **144**, 278-287.
- [28] Scherfler C, Seppi K, Mair KJ, Donnemiller E, Virgolini I, Wenning GK, Poewe W (2012) Left hemispheric predominance of nigrostriatal dysfunction in Parkinson's disease. *Brain* **135**, 3348-3354.
- [29] Fiorenzato E, Antonini A, Bisiacchi P, Weis L, Biundo R (2021) Asymmetric dopamine transporter loss affects cognitive and motor progression in Parkinson's disease. *Mov Disord* **36**, 2303-2313.

- [30] Horsager J, Andersen KB, Knudsen K, Skjaerbaek C, Fedorova TD, Okkels N, Schaeffer E, Bonkat SK, Geday J, Otto M, Sommerauer M, Danielsen EH, Bech E, Kraft J, Munk OL, Hansen SD, Pavese N, Goder R, Brooks DJ, Berg D, Borghammer P (2020) Brain-first versus body-first Parkinson's disease: A multimodal imaging case-control study. *Brain* **143**, 3077-3088.
- [31] Morrish PK, Sawle GV, Brooks DJ (1996) An [18F]dopa-PET and clinical study of the rate of progression in Parkinson's disease. *Brain* **119**(Pt 2), 585-591.
- [32] Nandhagopal R, Kuramoto L, Schulzer M, Mak E, Cragg J, Lee CS, McKenzie J, McCormick S, Samii A, Troiano A, Ruth TJ, Sossi V, de la Fuente-Fernandez R, Calne DB, Stoessl AJ (2009) Longitudinal progression of sporadic Parkinson's disease: A multi-tracer positron emission tomography study. *Brain* **132**, 2970-2979.
- [33] Hsiao IT, Weng YH, Hsieh CJ, Lin WY, Wey SP, Kung MP, Yen TC, Lu CS, Lin KJ (2014) Correlation of Parkinson disease severity and 18F-DTBZ positron emission tomography. *JAMA Neurol* **71**, 758-766.
- [34] Pineda-Pardo JA, Sanchez-Ferro A, Monje MHG, Pavese N, Obeso JA (2022) Onset pattern of nigrostriatal denervation in early Parkinson's disease. *Brain* **145**, 1018-1028.
- [35] Knudsen K, Fedorova TD, Horsager J, Andersen KB, Skjaerbaek C, Berg D, Schaeffer E, Brooks DJ, Pavese N, Van Den Berge N, Borghammer P (2021) Asymmetric dopaminergic dysfunction in brain-first versus body-first Parkinson's disease subtypes. *J Parkinsons Dis* **11**, 1677-1687.
- [36] Postuma RB, Adler CH, Dugger BN, Hentz JG, Shill HA, Driver-Dunckley E, Sabbagh MN, Jacobson SA, Belden CM, Sue LI, Serrano G, Beach TG (2015) REM sleep behavior disorder and neuropathology in Parkinson's disease. *Mov Disord* **30**, 1413-1417.
- [37] Booij J, Kemp P (2008) Dopamine transporter imaging with [(123)I]FP-CIT SPECT: Potential effects of drugs. *Eur J Nucl Med Mol Imaging* **35**, 424-438.
- [38] Moore RY, Whone AL, Brooks DJ (2008) Extrastriatal monoamine neuron function in Parkinson's disease: An 18F-dopa PET study. *Neurobiol Dis* **29**, 381-390.
- [39] Qamhawi Z, Towey D, Shah B, Pagano G, Seibyl J, Marek K, Borghammer P, Brooks DJ, Pavese N (2015) Clinical correlates of raphe serotonergic dysfunction in early Parkinson's disease. *Brain* **138**, 2964-2973.